Toshibumi Kinoshita
Toshihide Ogawa
Yasuji Yoshida
Hajime Tamura
Hirotsugu Kado
Toshio Okudera

Curvilinear T1 hyperintense lesions representing cortical necrosis after cerebral infarction

T. Kinoshita (✉) · H. Tamura
H. Kado · T. Okudera
Department of Radiology,
Research Institute of Brain and Blood
Vessels-Akita, Akita, Japan
E-mail: kino@grape.med.tottori-u.ac.jp
Tel.: +81-859-34-8125
Fax: +81-859-34-8188

T. Ogawa
Division of Radiology,
Department of Pathophysiological and
Therapeutic Science, Faculty of Medicine,
Tottori University, 36-1 Nishi-cho,
Yonago, Tottori 683-8504, Japan

Y. Yoshida
Department of Pathology,
Research Institute of Brain and Blood
Vessels-Akita, Akita, Japan

Abstract Curvilinear T1 hyperintense lesions in the cerebral cortex in patients with subacute infarction were investigated for: (1) the presence or absence of T2* hypointensity and (2) correlations with neuropathologic findings. Thirty-six consecutive patients with subacute to chronic embolic infarction, in whom curvilinear hyperintense lesions in the infarcted cortex were seen on T1-weighted images, underwent echo-planar gradient-echo (GRE-EPI) T2*-weighted imaging. GRE-EPI T2*-weighted imaging revealed no evidence of hemorrhage within the curvilinear T1 hyperintense lesions of the cerebral cortex in all of the patients. In 11 of the 36 patients, focal hypointense lesions were seen in the depth of infarcted gyri on GRE-EPI T2*-weighted images. In the remaining 25 patients, no T2* hypointensities were seen in the infarct zone. Pathological correlation was performed in a patient with middle cerebral artery infarction and curvilinear hyperintense lesions on postmortem T1-weighted images. In the autopsied brain, curvilinear T1 hyperintense lesions corresponded to necrosis of all the cortical layers on histological examination. These data suggest that curvilinear hyperintense lesions in the cerebral cortex on T1-weighted images during the subacute to chronic period of cerebral infarction may not represent hemorrhage.

Keywords Cerebral infarction ·
Cortical necrosis · MRI ·
Signal intensity

Introduction

On T1-weighted MR images, hyperintense lesions of the cerebral cortex are seen during the subacute stage of cerebral infarction [1–5]. Curvilinear cortical T1 hyperintense lesions begin to appear about two weeks after the onset, are prominent at one to two months, and then become less obvious, but persist for up to 1.5 years [3–5]. These hyperintense lesions have been suggested to represent cortical laminar necrosis, as seen in hypoxic brain injury [3–7]. It remains to be determined whether T1 shortening can be caused by a non-heme mechanism.

Echo-planar gradient-recalled echo (GRE-EPI) T2*-weighted imaging is sensitive for the early detection of hemorrhagic conversion of cerebral infarction [8, 9]. GRE-EPI T2*-weighted imaging can depict hemorrhages better than CT [8]. Subacute hematoma, even very small petechial lesions, present as markedly hypointense areas on GRE-EPI T2*-weighted images [10, 11].

The purpose of the present study was to characterize nonhemorrhagic T1 hyperintense lesions by the absence of hypointense area on GRE-EPI T2*-weighted images. To the best of our knowledge, pathological correlations of T1 hyperintense lesions due to embolic infarction have rarely been reported [12]. We describe the pathological correlates of T1-weighted hyperintense cortical lesions in one histologically proven case of cerebral infarction.

Materials and methods

We retrospectively reviewed 36 consecutive patients (16 women, 20 men, aged 50–87 years) with hemispheric embolic infarction, in whom curvilinear hyperintense lesions were noted in the cerebral cortex on T1-weighted MR images. MR imaging was performed 13 days to 4 months after onset. MR images were obtained using a 1.5-T superconducting unit with echo-planar capabilities. In all cases, axial spin–echo T1-weighted images (TR/TE/excitations, 665 ms/14 ms/2; slice thickness/interslice gap, 5 mm/1 mm; field of view, 23 cm; matrix, 224×256), axial fast spin–echo T2-weighted images (TR/TE/excitations, 3,600 ms/96 ms/2; slice thickness/interslice gap, 5 mm/1 mm; field of view, 23 cm; matrix, 224×256), and GRE-EPI T2*-weighted images (TE/excitations, 25 ms/1; flip angle 90°, slice thickness/interslice gap, 5 mm/1 mm; field of view, 23 cm; matrix, 128×128) were obtained.

MR images were evaluated by two of the authors (T.K., T.O.) to determine the presence or absence of T2*-hypointense lesions within the infarct. If a hypointense area was noted on GRE-EPI T2*-weighted images, the location of the T2*-hypointense area was compared with that of T1 hyperintense lesion.

In addition, our MR-pathologic correlation study was performed in an 83-year-old woman who eventually died of renal infarction. MR imaging was undertaken with a 0.5-T superconducting unit. Axial spin–echo T1-weighted images (TR/TE/excitations, 460 ms/20 ms/2;

field of view, 25 cm; matrix, 256×256) were obtained with 8-mm slices and no interslice gap. MR images of the formalin-fixed brain (postmortem MR images) were also obtained with the brain positioned in the head coil in a standard way. The autopsy specimens were stained with hematoxylin–eosin to detect the infarct in a standard fashion. Specimens were also stained with Prussian blue reaction to determine whether iron deposits were present. Histopathologic findings were compared with the final antemortem MR images and the postmortem MR images.

Results

In 25 of the 36 patients, anemic infarction was diagnosed because of the absence of T2*-hypointense areas, while T1-weighted images showed curvilinear hyperintense lesions in the cerebral cortex (Fig. 1). In the remaining 11 patients, hemorrhagic conversion was noted because of the presence of T2*-hypointense areas. The hypointense areas of GRE-EPI T2*-weighted images did not correspond in their distribution to the hyperintense lesions on T1-weighted images (Fig. 2). Curvilinear T1 hyperintense lesions near the surface of the cerebral cortex did not show hypointensity on GRE-EPI T2*-weighted images in any of the patients, while there were signal intensity changes in the depth of infarcted gyri, which gave hypointensity on GRE-EPI T2*-weighted images and hyperintensity on T1-weighted images.

Pathological correlation could be done in an 83-year-old woman with cardioembolic cerebral infarction in the territory of the right middle cerebral artery. She presented with left hemiparesis, and her medical history included atrial fibrillation. T1-weighted imaging obtained at 27 days after the onset showed curvilinear hyperintense lesions in the cerebral cortex (Fig. 3a). She died at 94 days after MR examination. T1-weighted

Fig. 1a–c A 70-year-old man with nonhemorrhagic cerebral infarction in the territory of the right middle cerebral artery, at 28 days after the onset. **a** T1-weighted image shows curvilinear hyperintense lesions in the cerebral cortex. **b** T2-weighted image shows relatively low signal cortical lesions and hyperintense area in the white matter. **c** GRE-EPI T2*-weighted image reveals no noticeable area of hypointensity in the infarct. A small hypointense area representing old lacunar hemorrhage is seen in the right thalamus
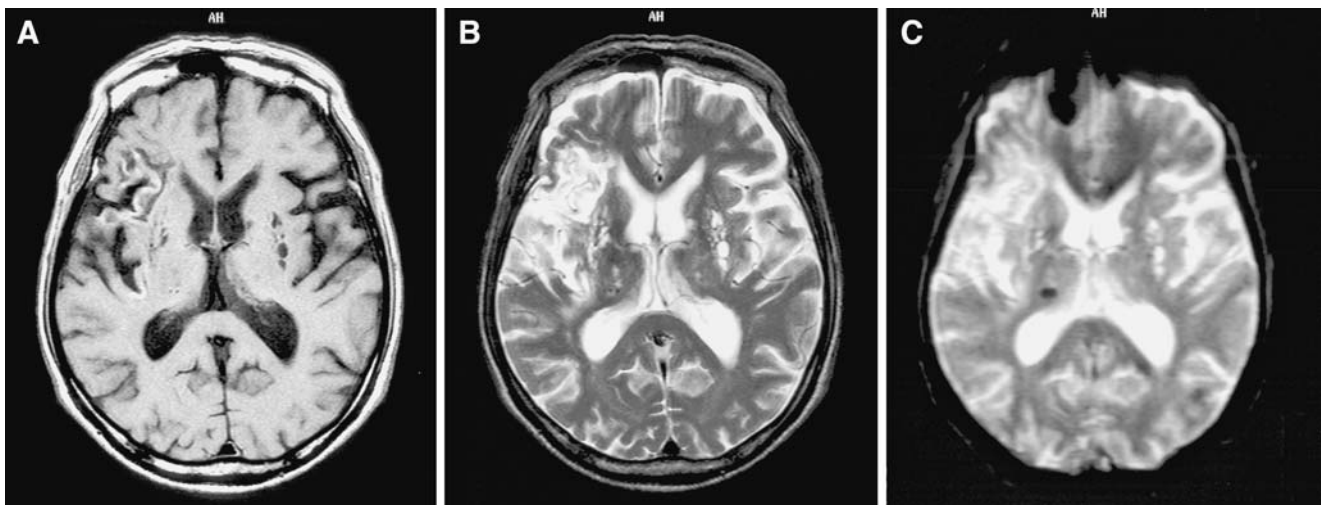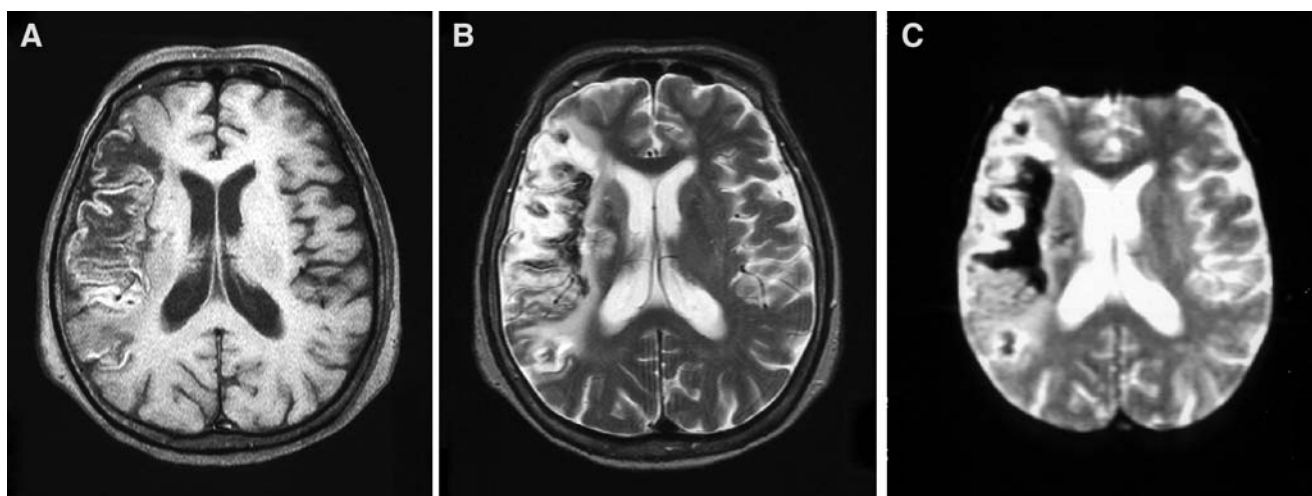
Fig. 2a–c A 73-year-old woman with cerebral infarction with hemorrhagic conversion in the territory of the right middle cerebral artery, at 37 days after the onset. a T1-weighted image shows hyperintense lesions in the cerebral cortex. b T2-weighted image shows hypointense lesions in the deep parts of infarcted gyri. c GRE-EPI T2*-weighted image reveals prominently hypointense lesions in the deep parts of infarcted gyri. Hypointense suscepti-bility artifact is not evident at the crests of the infarcted gyri

imaging of the brain at autopsy showed curvilinear hy-perintense lesions in the cerebral cortex (Fig. 3b). Au-topsy disclosed infarction of the right cerebral hemisphere (Fig. 3c). Histologically, necrotic debris fil-led the entire cortex in the infarcted area (Fig. 3d). Small numbers of fat-laden macrophages were present. Abundant reactive astrocytes encircled the necrotic zone of the cortex. The necrotic debris in the infarcted cortex was negative for Prussian blue staining, suggesting that extravasation of blood had not occurred.

Discussion

A significant percentage of initially anemic infarcts un-dergo spontaneous hemorrhagic transformation, which can take one of two forms, i.e., multiple grossly visible petechiae that usually remain confined to the gray matter, or massive hemorrhage that entirely replaces the originally ischemic tissues [13]. Even in the area of anemic infarction, microscopically visible microhemor-rhages can be seen and red blood cell extravasation occurs to some degree even in a grossly anemic infarct [1, 14].

GRE-EPI T2*-weighted imaging is uniquely sensitive for detecting asymptomatic old hemosiderin deposits [15, 16]. GRE-EPI T2*-weighted imaging has also been proved to be very sensitive for intraparenchymal blood, even in the acute stage, since the low signal intensity of intraparenchymal hematomas at GRE-EPI

T2*-weighted imaging can be explained by the presence of paramagnetic blood breakdown products, such as deoxyhemoglobin and methemoglobin, which create magnetic susceptibility effects. T2*-weighted imaging can detect subacute small bleeds [10, 11]. Furthermore, GRE-EPI T2*-weighted imaging can be used as a tool for evaluating hemorrhagic conversion in the subacute stage of cerebral infarction [8, 9]. T2*-hypointensity can be detected in almost all the stages of the breakdown of hemoglobin. We found curvilinear cortical T1-hyperin-tensities with no evidence of T2*-hypointensity, sug-gesting that shortening of T1 relaxation time may be mediated by a non-heme mechanism.

Anemic infarction describes a zone of coagulation necrosis or pan-necrosis that is often secondary to arterial occlusion [12, 17–19]. The appearance of areas of coagulation necrosis is delayed. In the chronic stage, reabsorption of necrotic debris takes place, and the ne-crotic tissues are replaced by a cavity filled with fluid [18, 19]. Our pathological correlation study demonstrated that curvilinear cortical lesions corresponded to areas of severe pancortical necrosis that were tantamount to infarction. The cellular infiltrate replacing the neuronal layers comprised a mixture of astrocytes and macro-phages.

The MR intensity patterns of cortical necrosis due to cerebral infarction are similar to those of cortical lami-nar necrosis in patients with hypoxic brain damage, but there are several distinguishing features. First, cerebral infarction causes necrosis of the entire thickness of the cerebral cortex, while cortical laminar necrosis only in-volves the most vulnerable layers. The third of the six cortical layers is the most vulnerable, while the fifth and sixth layers are somewhat less vulnerable, and the sec-ond and fourth layers are even more resistant [5]. An intracortical band of necrosis caused by focal infarction tends to be broad. Pseudolaminar necrosis also occurs, especially at the periphery of the infarcted areas.

Fig. 3a–d An 83-year-old woman with cerebral infarction in the territory of the right middle cerebral artery. **a** T1-weighted image obtained 27 days after the onset shows curvilinear hyperintense lesions in the cerebral cortex. **b** Postmortem T1-weighted image shows curvilinear hyperintense lesions in the cerebral cortex. **c** Pathologic specimen obtained in the area that corresponds to **b** shows infarction in the territory of the right middle cerebral artery. Infarcted white matter with cystic change is pale. A relatively dense cortical lesion in the infarct zone corresponds to the curvilinear hyperintense area on T1-weighted images. **d** Histological examination reveals necrotic debris replacing the entire cerebral cortex. A thin rim of preserved subpial tissue overlies a zone of cortex in which necrotic debris is identified. A cavity surrounded by a dense layer of reactive astrocytes is noted in the white matter
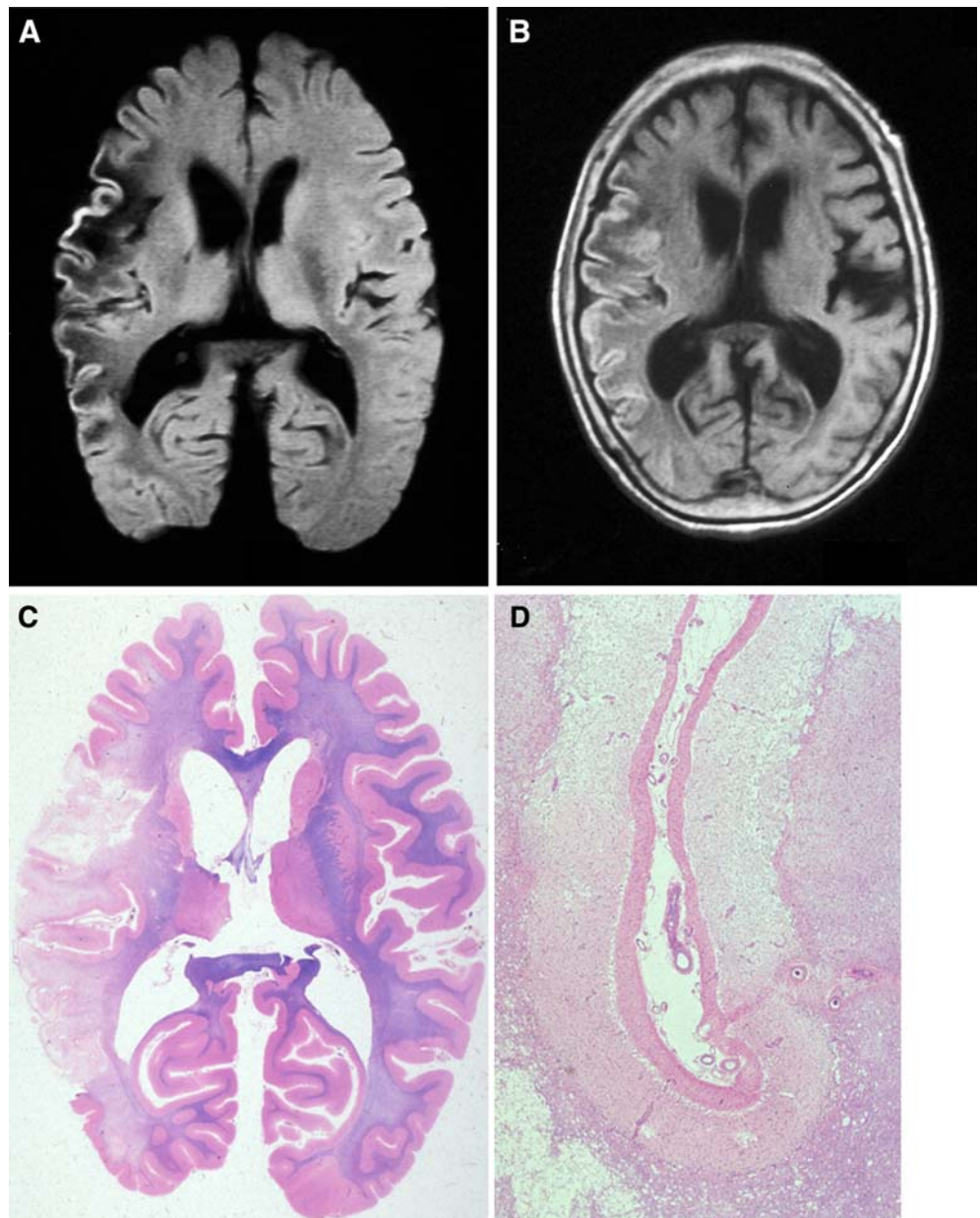
However, we cannot discriminate laminar necrosis from pseudolaminar necrosis, based on the width of cortical T1-hyperintense lesions. Second, cortical necrosis tends to occur along the crests of the gyri, while cortical involvement due to hypoxic brain injury is predominantly adjacent to the depths and sides of the cortical sulci rather than over the crests of the gyri. Third, delayed cystic change of the white matter occurs after cerebral infarction, whereas degenerative white matter changes including iron deposition are seen in the chronic stage of hypoxic brain damage [6].

Our MR-pathological correlation study in an autopsied patient with chronic cerebral infarction demonstrated that cortical curvilinear lesions showing hyperintensity on T1-weighted images corresponded to necrotic debris in the entire cortex. A concentrated protein solution in the necrotic debris is likely to show a shortened T1 relaxation time due to the macromolecular hydration effect. Negative for iron with Prussian blue staining indicates that hemorrhage did not occur. Although high cellularity may be attributed to T1-shortening, a mixture of astrocytes and macrophages was seen at the periphery of the infarcted area. Thereafter, we suggest that a main cause of T1 shortening caused in the infarcted cortex was denatured protein in the necrotic debris. Since cortical T1 hyperintensity is marked during the subacute period, biochemical factors, including paramagnetic compounds such as manganese ions,

and free radicals produced by macrophages, may also contribute to T1-shortening in the earlier phase [20, 21]. Alternatively, deposition of fat-laden macrophages, or cellular components of necrotic tissue, may be implicated in T1 shortening [12, 22]. Thus, a T1 high signal is likely to represent the consequence of acute necrosis.

Hemorrhagic conversion of anemic infarction has become the focus of great interest since this may carry a higher risk of clinical deterioration. The incidence of hemorrhagic conversion correlates with the volume of the brain lesion and the administration of anticoagulants [23, 24]. GRE-EPI T2*-weighted imaging should be preferred over T1-weighted imaging for the detection of post-ischemic cerebral hemorrhage.

In conclusion, curvilinear hyperintense lesions in the cerebral cortex on T1-weighted MR images during the subacute to chronic period of embolic infarction may not represent hemorrhage. GRE-EPI T2*-weighted imaging, with its ability to detect hemoglobin degradation products, is a highly sensitive and specific tool for the identification of hemorrhagic conversion. Denatured protein in necrotic debris might be the main cause of T1 shortening on MR images of nonhemorrhagic cerebral infarcts.

References

1. Nabatame H, Fujimoto N, Nakamura K et al. (1990) High intensity areas on noncontrast T1-weighted MR images in cerebral infarction. J Comput Assist Tomogr 14:521–526
2. Boyko OB, Burger PC, Shelburne JD, Ingram P (1992) Non-heme mechanisms for T1 shortening: pathologic, CT, and MR elucidation. Am J Neuroradiol 13:1439–1445
3. Komiyama M, Nakajima M, Yasui T (1997) Cortical laminar necrosis in brain infarcts: chronological changes on MRI. Neuroradiology 39:474–479
4. Komiyama M, Nakajima H, Nishikawa M, Yasui T (1998) Serial MR observation of cortical laminar necrosis caused by brain infarction. Neuroradiology 40:771–777
5. Siskas N, Lefkopoulos A, Ioannidis I, Charitandi A, Dimitriadis AS (2003) Cortical laminar necrosis in brain infarcts: serial MRI. Neuroradiology 45:283–288
6. Takahashi S, Higano S, Ishii K, Matsumoto K, Sakamoto K, Iwasaki Y, Suzuki M (1993) Hypoxic brain damage: cortical laminar necrosis and delayed changes in white matter at sequential MR imaging. Radiology 189:449–456
7. Sawada H, Udaka F, Seriu N, Shindou M, Kameyama M, Tsujimura M (1990) MRI demonstration of cortical laminar necrosis and delayed white matter injury in anoxic encephalopathy. Neuroradiology 32:319–321
8. Arnould MC, Grandin CB, Peeters A, Cosnard G, Duprez TP (2004) Comparison of CT and three MR sequences for detecting and categorizing early (48 hours) hemorrhagic transformation in hyperacute ischemic stroke. Am J Neuroradiol 25:939–944
9. Hermier M, Nighoghossian N, Derex L, Berthezène Y, Blanc-Lasserre K, Trouillas P, Froment JC (2001) MRI of acute post-ischemic cerebral hemorrhage in stroke patients: diagnosis with T2*-weighted gradient-echo sequences. Neuroradiology 43:809–815
10. Ripoll MA, Siosteen B, Hartman M, Raininko R (2003) MR detectability and appearance of small experimental intracranial hematomas at 1.5 T and 0.5 T. A 6–7 month follow-up study. Acta Radiol 44:199–205
11. Ripoll MA, Stenborg A, Sonninen P, Terent A, Rininko R (2004) Detection and appearance of intraparenchymal haematomas of the brain at 1.5 T with spin-echo, FLAIR and GE sequences: poor relationship to the age of the haematoma. Neuroradiology 46:435–443
12. Castillo M, Scatliff JH, Kwock L, Green JJ, Suzuki K, Chancellor K, Smith JK (1996) Postmortem MR imaging of lobar cerebral infarction with pathologic and in vivo correlation. Radiographics 16:241–250
13. Bogousslavsky J, Regli F, Uske A et al. (1991) Early spontaneous hematoma in cerebral infarct: is primary cerebral hemorrhage overdiagnosed? Neurology 41:837–840
14. Okazaki H (1989) Cerebrovascular disease. In: Okazaki H (ed) Fundamentals of neuropathology, 2nd edn. Igaku-shoin, Tokyo, pp 27–94
15. Kinoshita T, Okudera T, Tamura H, Ogawa T, Hatazawa J (2000) Assessment of lacunar hemorrhage associated with hypertensive stroke by echo-planar gradient-echo T2*-weighted MRI. Stroke 31:1646–1650
16. Nighoghossian N, Hermier M, Adeleine P et al. (2002) Old microbleeds are a potential risk factor for cerebral bleeding after ischemic stroke A gradient-echo T2*-weighted MRI study. Stroke 33:735–742
17. Garcia JH, Liu KF, Ye ZR, Gutierrez JA (1997) Incomplete infarct and delayed neuronal death after transient middle cerebral artery occlusion in rats. Stroke 28:2303–2310
18. Mirra SS, Hyman BT (2002) Ageing and dementia. In: Graham DI, Lantos PL (eds) Greenfield's neuropathology, 7th edn. Arnold, London, pp 195–272
19. Graham DI (1992) Hypoxia and vascular disorders. In: Adams JU, Duchen LW (eds) Greenfield's neuropathology, 5th edn. Arnold, London, pp 153–268
20. Fujioka M, Okuchi K, Hiramatsu KI, Sakaki T, Sakaguchi S, Ishii Y (1997) Specific changes in human brain after hypoglycemic injury. Stroke 28:584–587
21. Kim GW, Kondo T, Noshita N, Chan PH (2002) Manganese superoxide dismutase deficiency exacerbates cerebral infarction after focal cerebral ischemia/reperfusion in mice. Implications for the production and role of superoxide radicals. Stroke 33:809–815
22. Mabuchi T, Kitagawa K, Ohtsuki T et al. (2000) Contribution of microglia/macrophages to expansion of infarction and response of oligodendrocytes after focal cerebral ischemia in rats. Stroke 31:1735–1743
23. Lyden PD, Zivin JA (1993) Hemorrhagic transformation after cerebral ischemia: mechanisms and incidence. Cerebrovasc Brain Metab Rev 5:1–16
24. Calandre L, Ortega JF, Bermejo F (1984) Anticoagulation and hemorrhagic infarction in cerebral embolism secondary to rheumatic heart disease. Arch Neurol 41:1152–1154